

# Experimental investigation about influences of longitudinal-mode structure of pumping source on a Ti:sapphire laser

Huadong Lu, Jing Su,\* Changde Xie, and Kunchi Peng

State Key Laboratory of Quantum Optics and Quantum Optics Devices, Institute of Opto-Electronics, Shanxi University, Taiyuan, Shanxi 030006, China

\* [jingsu@sxu.edu.cn](mailto:jingsu@sxu.edu.cn)

**Abstract:** Using a multi-longitudinal-mode (MLM) and a single-longitudinal-mode (SLM) all-solid-state green lasers to be the pumping sources of a continuous-wave Ti:sapphire laser, respectively, the intensity-noise dependence of the Ti:sapphire laser on the longitudinal-mode structure of pumping sources is experimentally studied. The comparison between the theoretical prediction based on the quantum-mechanical model and the experimental measurement for the intensity-noise spectra is presented.

©2011 Optical Society of America

**OCIS codes:** (270.2500) Fluctuations, relaxations, and noise; (140.3515) Lasers, frequency doubled; (140.3560) Lasers, ring; (140.3590) Lasers, titanium.

---

## References and links

1. P. F. Moulton, "Spectroscopic and laser characteristics of Ti:Al<sub>2</sub>O<sub>3</sub>," *J. Opt. Soc. Am. B* **3**(1), 125–133 (1986).
2. S. Qamar, H. Xiong, and M. S. Zubairy, "Influence of pump-phase fluctuations on entanglement generation using a correlated spontaneous-emission laser," *Phys. Rev. A* **75**(6), 062305 (2007).
3. D. Wang, Y. Shang, Z. Yan, W. Wang, X. Jia, C. Xie, and K. Peng, "Experimental investigation about the influence of pump phase noise on phase-correlation of output optical fields from a non-degenerate parametric oscillator," *Europhys. Lett.* **82**(2), 24003 (2008).
4. D. Wang, Y. Shang, X. Jia, C. Xie, and K. Peng, "Dependence of quantum correlations of twin beams on the pump finesse of an optical parametric oscillator," *J. Phys. At. Mol. Opt. Phys.* **41**(3), 035502 (2008).
5. T. C. Ralph, C. C. Harb, and H. A. Bachor, "Intensity noise of injection-locked lasers: Quantum theory using a linearized input-output method," *Phys. Rev. A* **54**(5), 4359–4369 (1996).
6. C. C. Harb, T. C. Ralph, E. H. Huntington, D. E. McClelland, H.-A. Bachor, and I. Freitag, "Intensity-noise dependence of Nd:YAG lasers on their diode-laser pump source," *J. Opt. Soc. Am. B* **14**(11), 2936–2945 (1997).
7. Z. Jing, Z. Kuanshou, C. Yanli, Z. Tiancai, X. Changde, and P. Kunchi, "Intensity noise properties of LD pumped single-frequency ring laser," *Acta Opt. Sin.* **20**(10), 1311–1316 (2000).
8. Zhang, Y. Cheng, T. Zhang, K. Zhang, C. Xie, and K. Peng, "Investigation of the characteristics of the intensity noise of singly resonant active second-harmonic generation," *J. Opt. Soc. Am. B* **17**(10), 1695–1703 (2000).
9. M. Tsunekane, N. Taguchi, and H. Inaba, "High-power, efficient, low-noise, continuous-wave all-solid-state Ti:sapphire laser," *Opt. Lett.* **21**(23), 1912–1914 (1996).
10. J. Belfi, J. Galli, G. Giusfredi, and F. Marin, "Intensity noise of an injection-locked Ti:sapphire laser: analysis of the phase-noise-to-amplitude-noise conversion," *J. Opt. Soc. Am. B* **23**(7), 1276–1286 (2006).
11. S. Witte, R. T. Zinkstok, W. Hogervorst, and K. S. E. Eikema, "Control and precise measurement of carrier-envelope phase dynamics," *Appl. Phys. B* **78**(1), 5–12 (2004).
12. Y. Yamamoto, S. Machida, and O. Nilsson, "Amplitude squeezing in a pump-noise-suppressed laser oscillator," *Phys. Rev. A* **34**(5), 4025–4042 (1986).
13. A. Lucianetti, Th. Graf, R. Weber, and H. P. Weber, "Thermo-optical properties of transversely pumped composite YAG rods with Nd-doped core," *IEEE J. Quantum Electron.* **36**(2), 220–227 (2000).
14. L. Fengqin, Y. Lin, S. Yumei, Z. Yaohui, Z. Kuanshou, and P. Kunchi, "All-solid-state CW 12.9 W TEM<sub>00</sub> mode green laser," *Chin. J. Lasers* **36**(6), 1332–1336 (2009).
15. Y. Zheng, F. Li, Y. Wang, K. Zhang, and K. Peng, "High-stability single-frequency green laser with a wedge Nd:YVO<sub>4</sub> as a polarizing beam splitter," *Opt. Commun.* **283**(2), 309–312 (2010).
16. M. Bouafia, H. Bencheikh, L. Bouamama, and H. Weber, "M<sup>2</sup> quality factor as a key to mastering laser beam propagation," *Proc. SPIE* **5456**, 130–140 (2004).
17. L. Huadong, S. Jing, L. Fengqin, W. Wenzhe, C. Yougui, and P. Kunchi, "Compact, stable, tunable Ti:Sapphire laser," *Chin. J. Lasers* **37**(5), 1166–1171 (2010).
18. H. P. Yuen, and V. W. S. Chan, "Noise in homodyne and heterodyne detection," *Opt. Lett.* **8**(3), 177–179 (1983).
19. W. Yimin, L. Yupu, and Z. Yinghua, "Influence of the pump beam mode in a longitudinally pumped CW Ti:sapphire laser," *Chin. J. Lasers* **A23**(2), 111–116 (1996).

20. J. Harrison, A. Finch, D. M. Rines, G. A. Rines, and P. F. Moulton, "Low-threshold, cw, all-solid-state Ti:Al<sub>2</sub>O<sub>3</sub> laser," *Opt. Lett.* **16**(8), 581–583 (1991).
21. A. J. Alfrey, "Modeling of longitudinally pumped CW Ti:Sapphire laser oscillators," *IEEE J. Quantum Electron.* **25**(4), 760–766 (1989).
22. C. C. Harb, T. C. Ralph, E. H. Huntington, I. Freitag I, D. E. McClelland, and H. A. Bachor, "Intensity-noise properties of injection-locked lasers," *Phys. Rev. A* **54**(5), 4370–4382 (1996).
23. C. Becher, and K.-J. Boller, "Intensity noise properties of Nd:YVO<sub>4</sub> microchip lasers pumped with an amplitude squeezed diode laser," *Opt. Commun.* **147**(4-6), 366–374 (1998).
24. H. Nagai, M. Kume, I. Otha, H. Shimizu, and M. Kazumura, "Noise generation in laser diode-pumped solid state lasers due to mode hopping of pumping laser diodes," in *Conference on Lasers and Electro-Optics*, Vol. 12 of 1992 OSA Technical Digest Series (Optical Society of America, Washington, D. C., 1992), paper CWG 32.
25. T. Baer, "Large-amplitude fluctuations due to longitudinal mode coupling in diode-pumped intracavity-doubled Nd:YAG lasers," *J. Opt. Soc. Am. B* **3**(9), 1175–1180 (1986).

## 1. Introduction

All-solid-state continuous-wave (CW) single-frequency tunable Ti:sapphire lasers with compact configuration and high efficiency have been extensively applied to high-sensitive laser spectroscopy, quantum communications, high-precision interferometry and so on owing to their broad tunable wavelength range from 700 nm to 1000 nm [1]. Recent years, when Ti:sapphire lasers are used in the experimental researches of laser cooling of atoms, quantum optics and quantum information, more and more attentions have to be paid in reducing intensity noises of their output light since the extra noises on laser sources will severely influence the experimental results [2–4]. Ralph and Harb established a theoretical model based on quantum mechanics to express the effect of different noise sources on the intensity noises of the output light from lasers [5]. Successively, Harb et al. experimentally compared the intensity noises of two sets of Nd:YAG ring lasers pumped by a single-element diode laser (SEDL) or by a diode-laser array (DLA), respectively [6]. They showed that the intensity noise of the Nd:YAG laser depends on vacuum fluctuations as well as on pumping source noise and demonstrated that the semiclassical rate-equation model was not sufficient to describe the noise behavior of the lasers since it is unable to involve the influence of nonclassical vacuum fluctuations on the intensity-noise spectrum. Using the quantum mechanical model suggested in Ref [5], they successfully described the observed intensity-noise spectrum of the lasers. Later the model was used to study the intensity noise of LD-pumped Nd:YVO<sub>4</sub>, Nd:YAP lasers [7] and single-frequency-doubling lasers [8], respectively. In 1996, Masaki Tsunekane et al. compared the intensity noises of tunable Ti:sapphire lasers pumped by an Ar-ion laser with that pumped by an all-solid-state green laser and showed that the intensity noises of the output light from the Ti:sapphire laser pumped by Ar-ion laser was 2 orders of magnitude around 0.5 MHz higher than that pumped by the all-solid-state laser [9]. However, they didn't consider the influence of the longitudinal-mode construction of the pumping source. In 2006, Jacopo Belfi et al. studied the noise properties of an injection-locked Ti:sapphire laser and demonstrated the strong influence of the phase-noises of the injected seed-laser on the intensity noises of the output light [10]. In 2004, S. Witter et al. studied the influences of the pumping source on the carrier-envelope offset phase of a 10-fs pulse Ti:sapphire laser, and pointed out that the use of a single-longitudinal-mode pumping source is advantageous when the carrier-envelope phase stabilization is required [11]. So far, the influences of the longitudinal-mode structure of pumping sources on the operating characteristics of a CW single-frequency Ti:sapphire laser have not been discussed to the best of our knowledge.

To investigate the influences of the longitudinal-mode structure of the pumping sources on the intensity noises of the output light from a pumped CW Ti:sapphire laser, we design and build two sets of all-solid-state green lasers which have different configuration and longitudinal-mode structure: one with single-transverse-mode but multi-longitudinal modes (MLM) and another one with single-longitudinal-mode (SLM). The intensity noise spectra of the SLM and MLM and the pumped Ti:sapphire lasers are experimentally measured with self-homodyne detectors, respectively. The experimental results point out that the noise features of the output light of the Ti:sapphire laser pumped by the SLM system are significantly

improved in comparison with that pumped by the MLM system, and the pumping efficiency of the SLM system is much higher than that of the MLM system. When the MLM pumping system was replaced by the SLM pumping system, the intensity noise of the Ti:sapphire laser at the resonant relaxation oscillation (RRO) frequency was decreased from 24 dB to 19 dB, the critical frequency reaching the quantum noise limit (QNL) was reduced from 7 MHz to 2.5 MHz, and the threshold pumping power was decreased from 5.6 W to 2.1 W. By means of the transfer-function-type theories [12] and the solutions developed by Ralph et al. [5] as well as the technique and the procedure outlined by Harb et al. [6], we obtained the theoretical predictions of the intensity noise spectra of the Ti:sapphire laser output based on the experimental parameters for the MLM and the SLM pumping systems, respectively. It is shown that the measured noise spectrum of the SLM pumping system basically agrees with the theoretical prediction but for the MLM pumping system, the agreement is not very well. The physical reasons of the disagreement will be analyzed in the section 4.

## 2. Experimental setups

At first, we briefly introduce the configurations of the MLM and SLM pumping systems (T-IVB and F-VII B, Yu Guang Co., Ltd.). Both of them are the intracavity frequency-doubled all-solid-state lasers with the fundamental wavelength of 1064 nm and doubling-frequency wavelength of 532 nm, the pumping sources of which are the CW fiber-bundled laser diodes (LDs) with the maximum output powers of 30 W for the MLM system and 60 W for the SLM system respectively (FB01L4511 and LIMO60-F400-DL 808-EX1126, LIMO Lissotschenko Mikrooptik GmbH). The diameter and the Numerical Aperture (NA) of the output coupling fiber for both LDs are 400  $\mu\text{m}$  and 0.22. The composite Nd:YVO<sub>4</sub>-YVO<sub>4</sub> rod consisting of the undoped end cap of 5 mm-length and 0.3 (0.2) at. % Nd-doped part of 8 (15) mm-length serves as the laser material for the MLM (SLM) system. The use of the composite laser crystal can minimize the effect of the thermal lens during the laser operation [13]. The lithium triborate LiB<sub>3</sub>O<sub>5</sub> (LBO) crystals with the dimensions of 3 mm  $\times$  3 mm  $\times$  22 mm and 3 mm  $\times$  3 mm  $\times$  18 mm are used for the frequency-doubling crystals in the MLM and the SLM system, respectively. The temperature of the LBO crystals is well controlled at the phase-matching temperature of 148 °C by a temperature controller with a precision of 0.1 °C (YG-1HC, Yu Guang Co., Ltd.). The resonant cavities of the MLM and the SLM systems are the three-mirror folded cavity [14] and the four-mirror ring cavity [15], respectively. To ensure unidirectional operation of the SLM system, an optical diode is inserted into its ring cavity. The maximal output power of 8 W at 532 nm is obtained under the LD pumping powers of 28 W (40 W) at 808 nm for the MLM (SLM) pumping system. Although both MLM and SLM systems are in a single-transverse-mode configuration, the measured quality-factors ( $M^2$ ) for the MLM and the SLM system at the same power of 8 W are less than 1.5 and 1.1, respectively. The larger the value of  $M^2$  is, the worse the quality of the beam transverse-mode is [16]. Thus the SLM system has smaller spot size at the focus in the Ti:sapphire crystal than that of the MLM system, which results in that the SLM system has higher pumping efficiency than that of the MLM system.

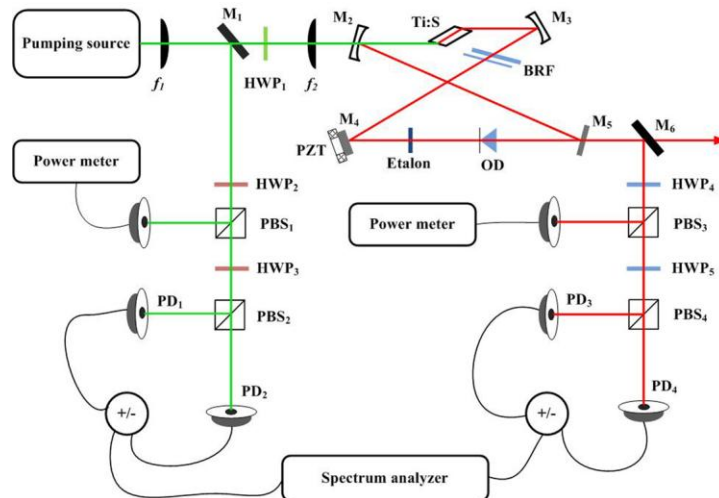


Fig. 1. (Color online) Experimental setup of measuring the intensity noise of all-solid-state CW single-frequency tunable Ti:sapphire laser.  $f_1$ ,  $f_2$ : Lens, BRF: Birefringent filter, OD: Optical diode, HWP<sub>1</sub>, HWP<sub>2</sub>, HWP<sub>3</sub>: Half-wave plate @ 532 nm, HWP<sub>4</sub>, HWP<sub>5</sub>: Half-wave plate @ 780 nm, PBS<sub>1</sub>, PBS<sub>2</sub>: Polarization-beam-splitter @ 532 nm, PBS<sub>3</sub>, PBS<sub>4</sub>: Polarization-beam-splitter @ 780 nm, PD<sub>1</sub>, PD<sub>2</sub>, PD<sub>3</sub>, PD<sub>4</sub>: Photo-detector.

The schematic diagram of the all-solid-state frequency-tunable and single-frequency CW Ti:sapphire laser (CTSL-I, Yu Guang Co., Ltd.) is shown in Fig. 1. The pumping source is the MLM or the SLM system. The lenses  $f_1$  and  $f_2$  form an optical coupling system to couple the pumping laser at 532 nm into the resonant cavity of the Ti:sapphire laser. A small part of the pumping laser is reflected by a beam-splitter ( $M_1$ ) for the measurements of the pumping noises and the pumping power. The ring resonator of the Ti:sapphire laser consists of four mirrors ( $M_2$ - $M_5$ ) in a figure-eight configuration [17]. A Brewster-cut gain material (Ti:sapphire crystal), a multi-plate birefringent filter (BRF) for tuning in a broad frequency-band, an optical diode (OD) for ensuring unidirectional operation of laser and an etalon for mode-selecting are placed in the resonator. The input coupler ( $M_2$ ) is coated with 95% transmission at 532 nm and the output coupler is coated with 3.1% transmission at 750-850 nm. The half-wave plate HWP<sub>1</sub> is used for the polarization alignment of the pumping laser with respect to the optical axis of the Ti:sapphire crystal. HWP<sub>3</sub> (HWP<sub>5</sub>), the polarizing-beam-splitter PBS<sub>2</sub> (PBS<sub>4</sub>) and the two silicon photo-diodes PD<sub>1</sub>, PD<sub>2</sub> (PD<sub>3</sub>, PD<sub>4</sub>) (S3399) compose the self-homodyne-detector for measuring the intensity noises of the pumping sources (Ti:sapphire laser). The optical signals detected by PD<sub>1</sub>-PD<sub>4</sub> are amplified by the integrated amplifiers (CLC425) and then the amplified photo currents of PD<sub>1</sub> and PD<sub>2</sub> (PD<sub>3</sub> and PD<sub>4</sub>) are combined with a negative or positive power combiner (+/-). The sum and the subtract photocurrents stand for the intensity noise and the corresponding quantum noise limit (QNL), respectively [18]. Finally, the noise spectra of the sum (subtract) photocurrents are analyzed by a spectral analyzer (SA) with the resolution bandwidth (RBW) of 30 kHz and the video bandwidth (VBW) of 30 Hz. HWP<sub>2</sub> (HWP<sub>4</sub>) and PBS<sub>1</sub> (PBS<sub>3</sub>) are used for controlling the laser power detected by the self-homodyne-detector and the power meter serves as the power monitor.

### 3. Experimental results

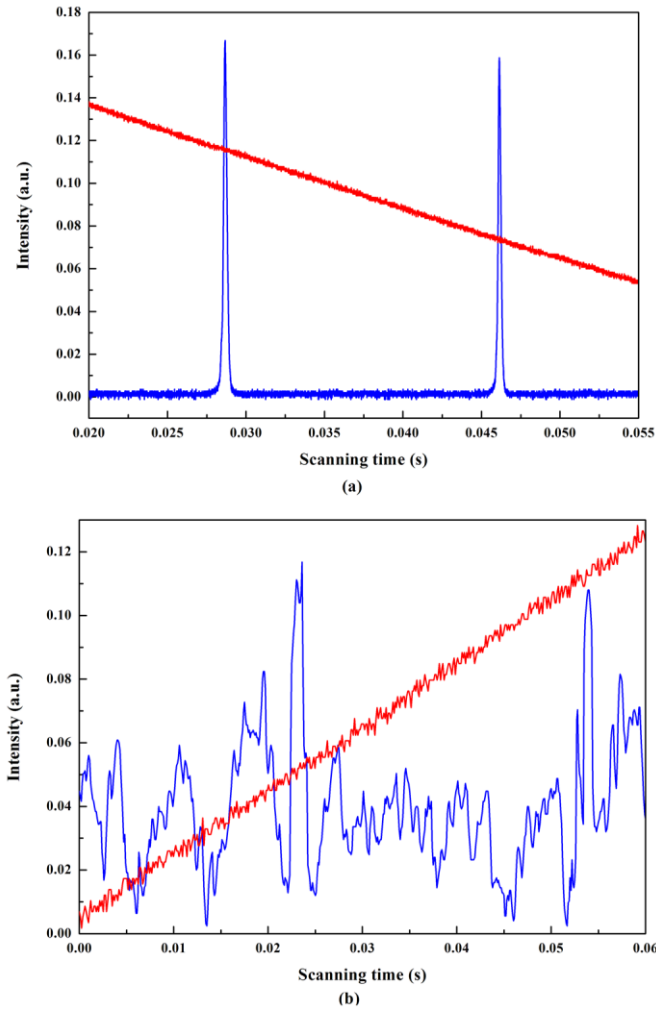


Fig. 2. (Color online) Longitudinal-mode structure of the pumping sources. (a) The SLM pumping system. (b) The MLM pumping system.

Figure 2(a) and 2(b) show the longitudinal-mode structures of the SLM (a) and the MLM (b) pumping source which are obtained by scanning the F-P interferometer. The MLM pumping system has complex and random longitudinal-mode configuration, thus it can be concluded that the severe mode-hopping and mode-competition effects exist in the pumping system which must significantly change the intensity noise property of the pumped Ti:sapphire laser.

The dependences of the output powers of the Ti:sapphire laser upon the pumping powers from the SLM (a) and the MLM (b) system are shown in Fig. 3. The threshold pumping powers for the SLM and MLM system are 2.1 W and 5.6 W, respectively. The obtained power of Ti:sapphire laser pumped by the SLM system is much higher than that pumped by the MLM system under same pumping power, that is because the transverse-mode quality of the SLM pumping system ( $M^2-1.1$ ) is much better than that of the MLM pumping system ( $M^2-1.5$ ), thus using the SLM pumping system we can obtain the smaller waist spot of the pumping light in the Ti:sapphire crystal and the higher pumping efficiency [19–21].

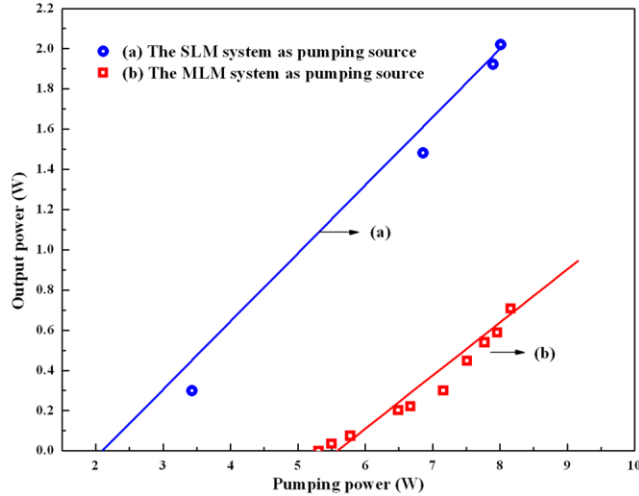


Fig. 3. (Color online) Output power of CW single-frequency tunable Ti:sapphire laser versus pumping power with different pumping sources. (a) The SLM system as pumping source. (b) The MLM system as pumping source.

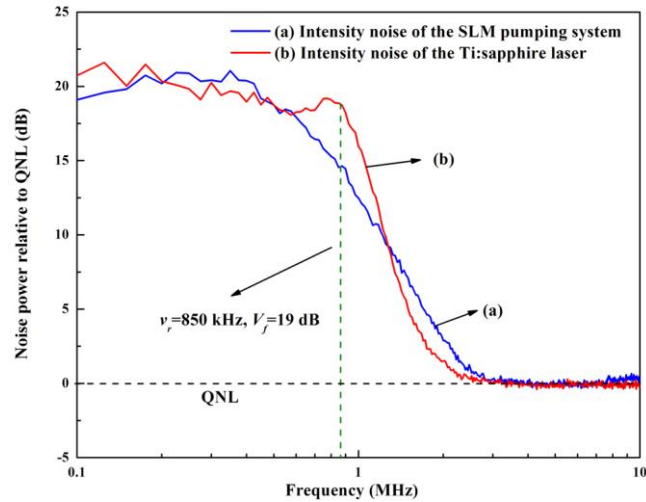


Fig. 4. (Color online) Intensity noise spectrum of the Ti:sapphire laser compared with that of the SLM pumping source. (a) Intensity noise of the SLM pumping system. (b) Intensity noise of the Ti:sapphire laser.

Figure 4 and 5 show the intensity noise spectra of the Ti:sapphire laser (b) compared with that of the pumping source (a) for the SLM (Fig. 4) and the MLM (Fig. 5) system, respectively. In the experiment the power of both SLM and MLM pumping systems with the wavelength of 532 nm is maintained at 8 W. Under this pumping level the output powers of the Ti:sapphire laser at 780 nm are about 2 W and 700 mW for the SLM and the MLM pumping system, respectively (See Fig. 3 for details). For performing the noise spectrum measurements in Fig. 4 and 5, the laser power injected into the homodyne detectors for all four optical beams is precisely adjusted to 30 mW with the intensity adjusters consisting of half-wave plates (HWP<sub>2</sub>-HWP<sub>5</sub>) and polarizing-beam-splitters (PBS<sub>1</sub>-PBS<sub>4</sub>). The optical attenuations for the pumping laser of 8 W and the Ti:sapphire laser of 2 W (700 mW) are 0.03/8 and 0.03/2 (0.03/0.7), respectively. The extra attenuation of the pumping power, which is 4-times (11.5-times) larger than the attenuation of the Ti:sapphire laser pumped by the SLM (MLM) system, has been taken into account in the noise spectra of Fig. 4 and 5 by appropriate

normalization [22]. The intensity-noise spectra are plotted relative to the QNL on a log-log scale, i. e.  $10\log_{10}(V_f)$  versus  $\log_{10}(\omega/2\pi)$  and 0 dB indicates that the noise level equals to the QNL. The frequency and the magnitude of the RRO for the Ti:sapphire laser pumped by the SLM (MLM) system are 850 kHz (725 kHz) and 19 dB (24 dB) above the QNL. At lower frequencies from 0.1 MHz to 0.6 MHz (close to the RRO) the intensity noise level of the Ti:sapphire laser pumped by the SLM system (Fig. 4(b)) is basically matched with that of the pumping source (Fig. 4(a)), but at the region higher than 0.6 MHz, the intensity noise profile of the Ti:sapphire laser is not in good agreement with that of the pumping source. For the MLM pumping system (Fig. 5(b)) only at the frequency region from 100 kHz to 175 kHz, the intensity noise level of the Ti:sapphire laser agrees with that of the pumping source (Fig. 5(a)). At frequencies higher than 175 kHz, the intensity noise of the Ti:sapphire laser is higher than that of the pumping source. It means that only at lower frequency the intensity noise from the pumping sources was transferred to the Ti:sapphire laser. In both SLM and the MLM systems, the intensity noise of Ti:sapphire laser reaches the QNL almost simultaneously with its pumping source [2.5 MHz for SLM (Fig. 4); 7MHz for MLM (Fig. 5)]. It should be mentioned that the measurements of the noise spectra are implemented from 0.1 MHz to 10 MHz in our experiments, since below 0.1 MHz the influences of the electronic noise from the detectors cannot be neglected and the gain of the electronic amplifiers is less than the required value, thus the observed noise spectra cannot represent the real intensity noise of the measured laser and above 10 MHz all noise spectra have reached the QNL.

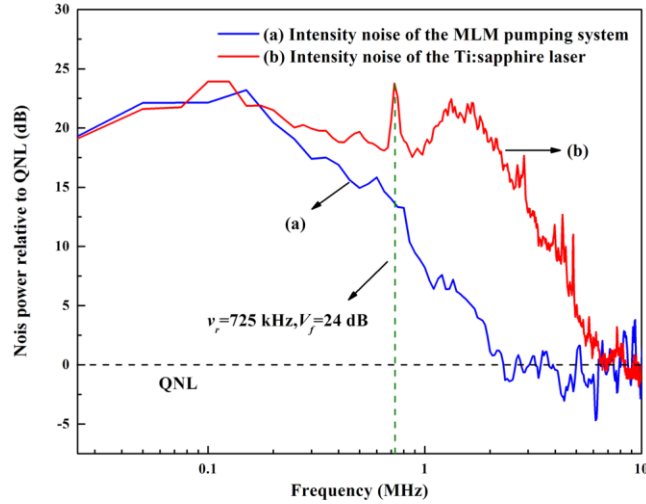


Fig. 5. (Color online) Intensity noise spectrum of the Ti:sapphire laser compared with that of the MLM pumping source. (a) Intensity noise of the MLM pumping system. (b) Intensity noise of the Ti:sapphire laser.

#### 4. Quantum theoretical prediction compared with experimental measurement

According to the transfer-function formula of the noise sources developed in Ref [5], the intensity-noise spectrum of the Ti:sapphire laser is expressed by  $V_f$ :

$$V_f = \left[ 1 + \frac{4\kappa_m^2(\omega^2 + \gamma_l^2) - 8\kappa_m\kappa G\alpha^2\gamma_l}{(\omega_r^2 - \omega^2)^2 + \omega^2\gamma_l^2} \right] V_{vac} + \left[ \frac{2\kappa_m G^2 \alpha^2 \Gamma}{(\omega_r^2 - \omega^2)^2 + \omega^2\gamma_l^2} \right] V_p + \left[ \frac{2\kappa_m G^2 \alpha^2 \gamma_l J_3}{(\omega_r^2 - \omega^2)^2 + \omega^2\gamma_l^2} \right] V_{spont} + \left[ \frac{2\kappa_m G J_3 [(\gamma_l + \Gamma)^2 + \omega^2]}{(\omega_r^2 - \omega^2)^2 + \omega^2\gamma_l^2} \right] V_{dipole} + \left[ \frac{4\kappa_m \kappa_l (\gamma_l^2 + \omega^2)}{(\omega_r^2 - \omega^2)^2 + \omega^2\gamma_l^2} \right] V_{losses} \quad (1)$$

where  $V_{\text{vac}}$ ,  $V_p$ ,  $V_{\text{spont}}$ ,  $V_{\text{dipole}}$  and  $V_{\text{losses}}$  are the noise inputs from vacuum noise entering the output coupler ( $V_{\text{vac}}$ ), pump-source intensity-noise spectrum ( $V_p$ ), spontaneous-emission noise ( $V_{\text{spont}}$ ), dipole fluctuation noise ( $V_{\text{dipole}}$ ) and noise introduced from intracavity losses ( $V_{\text{losses}}$ ), respectively.  $\omega$  is the noise frequency. The total cavity decay rate is  $2\kappa = 2(\kappa_m + \kappa_l)$ , the coefficients  $\kappa_m$  and  $\kappa_l$  derive from the output coupling and intracavity losses, respectively.  $\alpha^2$  is the intracavity photon number per atom of the lasing mode and is given by

$$\alpha^2 = \frac{\Gamma - \gamma_l J_3}{2\kappa} \quad (2)$$

$\Gamma$  is the pumping rate;  $J_3 = \frac{2\kappa}{G}$  is the occupation probability of the upper lasing level;  $G$  describes the coupling of the lasing transition to the laser mode and is proportional to the stimulated-emission cross section of the transition,  $\gamma_l$  is the rate of spontaneous emission from the upper lasing level.  $\omega_r = \sqrt{2\kappa G \alpha^2}$  is the frequency of the RRO.  $\gamma_l = G\alpha^2 + \gamma_l + \Gamma$  is the damping rate of the RRO.

The experimentally measured intensity-noise spectra of the Ti:sapphire laser for the SLM (a) and the MLM (b) pumping system compared with that of the theoretical prediction based on Eq. (1) [(c) for SLM and (d) for MLM] are shown in Fig. 6. The parameters for calculating the traces (c) and (d) are listed in Table 1.

**Table 1. Parameters used to calculate the noise spectra of Fig. 6(c) and 6(d)**

Parameter	Trace (c)	Trace (d)
$f_{\text{RRO}}$ (kHz)	850	725
$G$ ( $\text{s}^{-1}$ )	$1.89 \times 10^{11}$	$1.89 \times 10^{11}$
$2\kappa$ ( $\text{s}^{-1}$ )	$1.63 \times 10^7$	$1.63 \times 10^7$
$\gamma_l$ ( $\text{s}^{-1}$ )	$3.1746 \times 10^5$	$3.1746 \times 10^5$
$J_3$ per atom	$8.61 \times 10^{-5}$	$8.61 \times 10^{-5}$
$\alpha^2$ per atom	$9.23 \times 10^{-6}$	$7.21 \times 10^{-6}$
$N$ (atoms)	$9.25 \times 10^{16}$	$4.15 \times 10^{16}$
$\Gamma$ ( $\text{s}^{-1}$ )	178	145

These values presented here are determined by the technique outlined by Harb et al. [22]. For determining the predicted noise levels we determined the shape for one of the noise spectra firstly, then adjusted  $V_p$  and  $\Gamma$  to coincide with their measured values, and then produce all the other noise-spectra predictions. We selected the parameters to make the calculated RRO peak overlapping with the experimental RRO peak in both SLM and MLM pumping cases, respectively. The RRO frequency for the SLM pumping system is 850 kHz which is higher 125 kHz than that for the MLM pumping system (725 kHz). The magnitude of the RRO peak for the SLM pumping system is 19 dB above the QNL which is 5 dB lower than that of the MLM pumping system (24 dB). The results are in good agreement with the predictions of the quantum theory. Since the SLM pumping laser has a smaller waist spot and smaller mode volume in the Ti:sapphire crystal than that of the MLM pumping laser, the pumping rate of the SLM system must be faster than that of the MLM system under the same pumping power, which results in that the RRO frequency of the SLM system is higher and its RRO peaks is lower [23]. Compared with the RRO peak LD-pumped Nd:YAG laser presented in Ref [6], the width of RRO peak of Ti:sapphire laser is wider. That is because the life time of the laser upper level of the Ti:sapphire crystal is much shorter than that of Nd:YAG, thus the Ti:sapphire active medium has higher damping. For the SLM pumping system, the theoretical prediction (c) and the experimental noise spectrum (a) agree quite well at and beyond the RRO frequency. However, for the MLM pumping system, the predicted width of the RRO peak (d) is wider than that experimentally measured (b) and the measured noise spectrum beyond the RRO frequency is higher than that of theoretical prediction (d). We can see that beyond the RRO frequency the three traces of Fig. 6(a), 6(c) and 6(d) almost overlap, which means that just as the quantum theoretical prediction the noise spectrum of the Ti:sapphire laser pumped by the SLM system was not affected by the pumping noise beyond the RRO frequency. However, for the MLM system the intensity noise of Ti:sapphire laser (b) is much



higher. It means that the severe mode-hopping phenomena exist in the MLM pumping system which change significantly the intensity noise spectrum of Ti:sapphire laser as pointed out in Ref [6]. and [24].

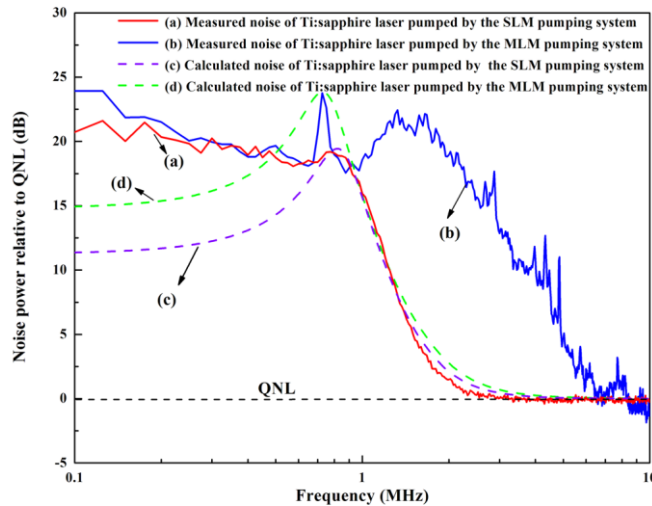


Fig. 6. (Color online) Ti:sapphire intensity noise spectra compared with the quantum prediction for the noise profile. (a), (b) Measured intensity noise profiles when the Ti:sapphire is pumped with the SLM and the MLM system, respectively. (c), (d) The corresponding calculated profiles.

From Fig. 4 and 5 we can see below the RRO frequency the intensity noise of the Ti:sapphire laser is mainly dominated by the noise spectrum of the pumping source. Not like the LD pumping source with white noises used in Ref [6], an intensity-noise distribution exists in both SLM and MLM pumping sources. When we drew the traces (c) and (d) of Fig. 6 using quantum model of Ref [5], only a value of the pumping noises was utilized and the distribution of the pumping noise did not considered. Thus the experimental spectra below the RRO are higher than that predicted theoretically and only around the RRO peak the prediction (c) for the SLM system agrees with the experimental trace (a). We believe that if the noise spectrum distribution of the pumping source is involved in the procedure for determining the predicted noise level, the quantum theoretical prediction will be in better agreement with the experimental results, especially for the SLM pumping system.

## 5. Conclusions

We experimentally studied the dependences of the Ti:sapphire laser upon the longitudinal-mode structure of the pumping sources. We found that when the single-longitudinal-mode laser serves as the pumping source not only the pumping efficiency is enhanced but also the noise feature of the Ti:sapphire laser is improved significantly. The laser systems with higher pumping efficiency and better intensity noise spectrum are very useful in scientific research and practical application. Our works provide feasible reference for designing and building high quality all-solid-state lasers.

The configuration of the laser transition levels of Ti:sapphire crystal is a broad-band two-level system. In this case the mode-hop and the mode-competition of the pumping laser will severely affect the operation of the pumped laser and increase the intensity noise of the output laser. On the other side in the MLM intracavity frequency-doubled Nd:YVO<sub>4</sub> pumping system with higher power of 8 W there are possibly the intercrossing saturation effect and the green problem [25] due to the existence of the frequency-doubling crystal. These effects are not involved in the Eq. (1), so the measured noise spectrum of the MLM pumped Ti:sapphire laser exists larger disagreement with that predicted theoretically. For the SLM pumping system, the noise spectrum at and after the RRO frequency is in good agreement with the quantum

theoretical prediction. But at lower frequency the experimental curve of Fig. 6(a) and the theoretical curve of Fig. 6(c) disagree, that is because the theoretical curve of Fig. 6(c) is drawn with a given value of pumping noises, which is taken only for reaching good agreement with the experimental measurement at the RRO frequency. However, the pumping noise is not the white noise and thus has different value at different frequency. The noise spectrum distribution of the pumping source was not involved in the calculation. We believe that if the noise distribution of the pumping source is considered, the theoretical calculation will be in better agreement with the experimental results for the SLM system. To the MLM system, more physical effects, such as mode-hop, mode-competition and so on should be involved in the theoretical formula for achieving better match between theory and experiment.

### **Acknowledgements**

This research was supported by the National Basic Research Program (973 Program) (No. 2010CB923103), NSFC Project for Excellent Research Team (No. 60821004), and the Key Program of NSFC (No. 60736040).